EasyChair Preprint

№ 8144

Nonlinear Trajectory Following Control for a Bio-Inspired Steerable Needle

Zejian Cui, Abdulhamit Donder and
Ferdinando Rodriguez Y Baena

EasyChair preprints are intended for rapid dissemination of research results and are integrated with the rest of EasyChair.

May 31, 2022

Nonlinear Trajectory Following Control for a Bio-Inspired Steerable Needle

Zejian Cui[1], Abdulhamit Donder[1], and Ferdinando Rodriguez Y Baena[1]

[1]*Department of Mechanical Engineering, Imperial College London,*
zejian.cui19@imperial.ac.uk; a.donder18@imperial.ac.uk; f.rodriguez@imperial.ac.uk

INTRODUCTION

Research in minimally invasive surgery has placed great focus on percutaneous intervention, leading to a booming research interest in steerable needles [1]. Such systems, compared with rigid needles, enjoy the advantage of following a curvilinear trajectory towards a target that lies under anatomical tissue surrounded by vessels while avoiding obstacles along the path. Amongst these, a bio-inspired programmable bevel-tip steerable needle (PBN) has been developed, which can steer in any direction in three-dimensional space without causing tissue damage due to torsion; its steering behaviour has been described by a mechanics-based model[2]. To further investigate needle tracking performance under the newly-developed needle model, this paper presents a tailored closed-loop controller which characterizes needle movement by applying an underactuated Autonomous Underwater Vehicle (AUV) model.

MATERIALS AND METHODS

A. Mechanics-based 3D PBN model

An interlocked four-segment steerable needle prototype that can steer in any direction in the 3D space within a predefined workspace has been developed and is currently undergoing preclinical trials on the ovine model. In [2], a mechanics-based Euler-Bernoulli beam model has been developed which establishes needle tip curvatures κ_P as a function of needle absolute offsets at the proximal end O and a vector of needle parameters μ. We define a nonlinear function f to calculate needle tip curvature κ_P as

$$\kappa_P = f(O, \mu) \tag{1}$$

It is also required that a permissibility condition must be satisfied so that the needle can move as a single body during insertion. Details are illustrated in [2], and here we summarize it as a function of needle absolute offsets as below

$$PM(O) = 1 \tag{2}$$

B. Trajectory following controller design

Based upon the aforementioned needle model, we have developed an overall trajectory following control strategy, which consists of a High-level controller (HLC) and a Low-level controller (LLC). The HLC takes inspiration from the AUV model, with the current and target needle poses as inputs and the linear moving velocity and rotational speeds around body frame axes as outputs. These HLC outputs are subsequently sent to the LLC, which interprets them into optimized needle inputs, with individual motion commands for each segment. The HLC considers the needle tip as an underactuated AUV following a reference trajectory and corrects the needle navigation path when it strays from the reference one. We assume there exists linear and rotational control inputs for the PBN except for the rotational speed around the needle axis, which is considered null. Built upon modified AUV kinematics and error dynamics as described in [3], the HLC control law is derived as follows. Denoting the needle tip is moving forward at the speed of v and steering around its body frame axes y_b and z_b at rates of ω_y and ω_z respectively, we have

$$\begin{cases} v = v_d + v_d(\cos\psi_e \cos\theta_e - 1) + \gamma^2 x_e \\ \vec{\omega} = \vec{\omega_d} + \vec{\mathbf{b_1^{-1}}}(\vec{\theta})(\vec{\mathbf{q}} + (\mathbf{B_1}(\vec{\theta_d}) - \mathbf{B_1}(\vec{\theta}))\vec{\omega_d} + \vec{\mathbf{p}}) \end{cases} \tag{3}$$

where $\gamma > 0$ is a non-negative HLC parameter, and $\vec{\mathbf{q}}$ and $\vec{\mathbf{p}}$ are as expressed as

$$\vec{\mathbf{q}} = [\, 0, -\frac{z_e v_d}{k_2}, \frac{y_e v_d \cos\theta_e}{k_3} \,]^T$$

$$\vec{\mathbf{p}} = [\, k_1 \sin\phi_e, k_2 \sin\theta_e, k_3 \sin\psi_e \,]^T$$

where k_1, k_2, k_3 are three other non-negative HLC parameters, definitions of other parameters can be directed to [3].

After the HLC generates outputs as v, ω_y and ω_z, v, the needle insertion speed, can be directly controlled via the needle actuation box as in [2], while ω_y and ω_z need to be further converted into executable needle inputs by the HLC. From curvature and rotation speed relationships, we first convert ω_y and ω_z desired needle tip curvatures $\kappa_d = [\, \kappa_{1_d}; \kappa_{2_d} \,]$, and based on (1) we let the LLC conduct an inverse mapping to generate needle offset movements commands. An open-source software tool CasADi, for numerical optimization and optimal control [4], is adopted. The process of finding needle

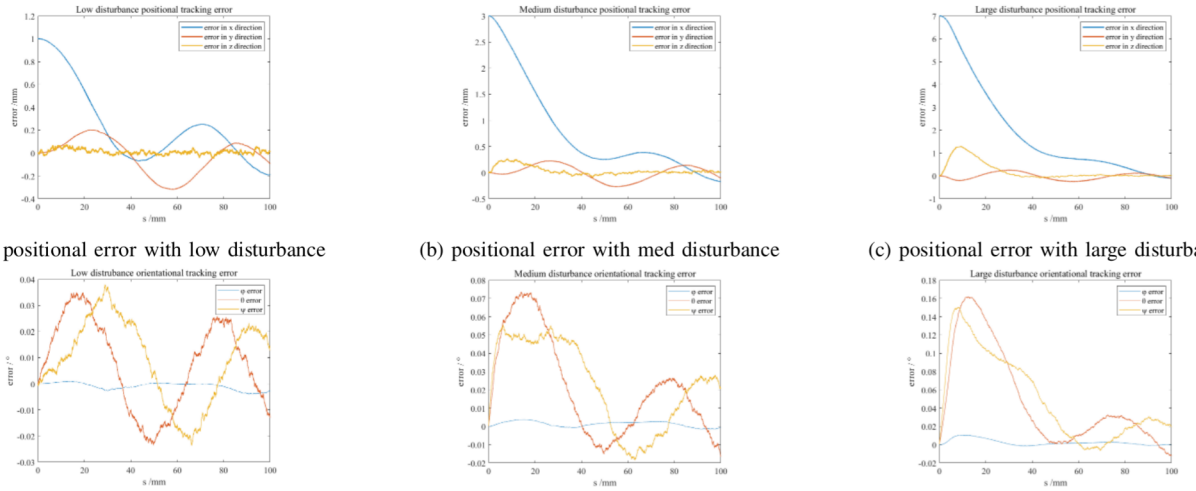

(a) positional error with low disturbance (b) positional error with med disturbance (c) positional error with large disturbance

(d) orientation error with low disturbance (e) orientation error with med disturbance (f) orientation error with large disturbance

Fig. 1 Euclidean errors during PBN navigation under different initial disturbances

offsets O corresponding to a reference tip curvature κ_d can be summarized into an optimization problem as

$$\text{minimize } J = \frac{1}{2} O^T Q O \tag{4}$$

$$\text{subject to } f(O, \mu) = \kappa_d \qquad PM(O) = 1 \tag{5}$$

where $O \in \mathbb{R}^{4\times1}$ is a column vector storing absolute offsets and $Q \in \mathbb{R}^{4\times4}$ is a weight matrix storing relative contributions of needle segments towards the overall control efforts.

C. Simulation

To analyze the performance of the combined control strategy, we present a trajectory tracking simulation conducted in Matlab 2020a (Mathworks inc.). Tracking performance is evaluated based on average positional errors between target and actual needle tip points along the course. A reference trajectory of insertion length s = 100 mm, whose curvatures along the path follow the following relationships, is selected.

$$\kappa_{ref}(s) = \begin{bmatrix} \kappa_{1_{ref}} \\ \kappa_{2_{ref}} \end{bmatrix} = 0.007 \begin{bmatrix} \cos(\frac{4\pi s}{100}) \\ \sin(\frac{4\pi s}{100}) \end{bmatrix} mm^{-1} \tag{6}$$

For the HLC, controller parameters are tuned experimentally and in this case we choose k_1 = 5, k_2 = 3.5, k_3 = 5, γ = 1. For the LLC, we consider driving each segment requires equal amount of effort and thus $\mathbf{Q} = \mathbf{I}^{4\times4}$. Needle parameters selected remain the same as in [2]. To simulate initial disturbances, three cases with disturbances on position and orientation being ± [1mm, 0°], ± [3mm, 1°] and ± [7mm, 3°], are exerted respectively. To simulate noises in needle position gathered by hypothetical position sensors, random noises with magnitude of 1mm and 5° are added.

RESULTS

The average Euclidean position error during trajectory tracking under low, medium and large disturbances were found to b 0.3480 mm, 0.8256 mm and 1.9043 mm respectively; the average Euclidean orientation errors in angle ϕ, θ and ψ were [-0.0009°,0.0077°,0.0092°], [0.0013°,0.0215°,0.0233°] and [0.0025°,0.0489°,0.0513°] respectively. The percentage of curvature references provided by the HLC to the LLC the value of which was found to exceed the maximum needle steering angle took up 99.84 %, 99.82 % and 99.87 % of all control steps under these three cases, respectively (shown in Figure 1).

DISCUSSION

The simulation results demonstrate that the combined controller is able to guide the PBN towards the reference trajectory under different initial perturbations and environmental disturbances, leading to a reduction in both position and orientation errors. However, we also notice that there always remains a certain amount of Euclidean error oscillating towards the end, which might be attributed to needle steerability limitations. This limitation implies that at each control step, the needle may fail to arrive at the desired state defined by the HLC and hence Euclidean errors persist and accumulate as the needle navigates. Experimental validation will follow in future work.

REFERENCES

[1] N. J. van de Berg, D. J. van Gerwen, J. Dankelman, and J. J. van den Dobbelsteen, "Design choices in needle steering—a review," *IEEE/ASME Transactions on Mechatronics*, vol. 20, no. 5, pp. 2172–2183, 2015.

[2] T. Watts, R. Secoli, and F. R. Y. Baena, "A Mechanics-Based Model for 3-D Steering of Programmable Bevel-Tip Needles," *IEEE Transactions on Robotics*, vol. 35, no. 2, pp. 371–386, 2019.

[3] Y. Nakamura and S. Savant, "Nonlinear tracking control of autonomous underwater vehicles," in *Proceedings 1992 IEEE International Conference on Robotics and Automation*, 1992, pp. A4–A9 vol.3.

[4] J. A. E. Andersson, J. Gillis, G. Horn, J. B. Rawlings, and M. Diehl, "CasADi – A software framework for nonlinear optimization and optimal control," *Mathematical Programming Computation*, In Press, 2018.